# From highly-collisional to collisionless fluid models

***Peter Hunana***
*Instituto de Astrofísica de Canarias, Tenerife, Spain*
*E. Khomenko (and her entire team), M. Collados, A. Tenerani, G. P. Zank*
*M. L. Goldstein, G. M. Webb, M. Velli, L. Adhikari*

When transitioning from highly-collisional to weakly-collisional systems, there is not enough force to keep the distribution function isotropic, which yields : **temperature anisotropy.**

In situ (solar wind) observational studies :

*Bale et al. 2009*

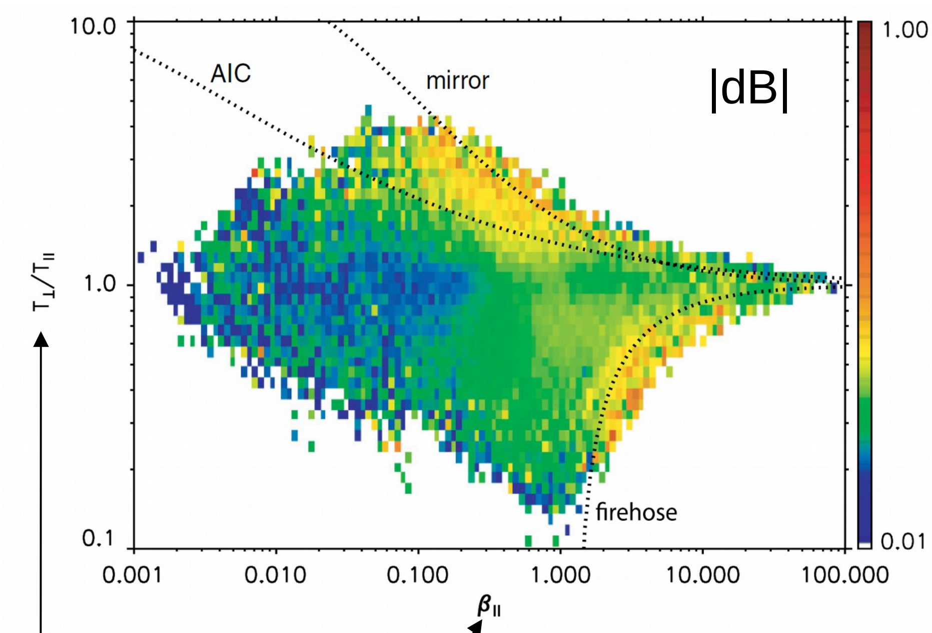


Parallel plasma beta

*Hellinger at al. 2006*

Ion-cyclotron anisotropy instability

mirror instability

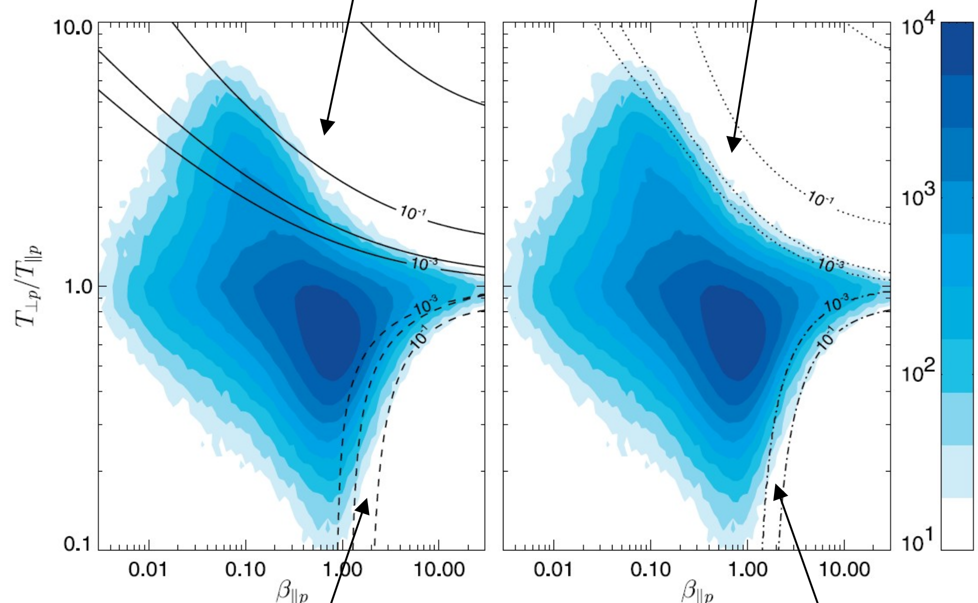


parallel firehose instability
(whistler mode)

oblique firehose instability
(oblique Alfven mode)

Temperature anisotropy. All highly-collisional (MHD-based) fluid models are just one line in these figures.

# Anisotropic (collisionless) fluid models

The simplest model is known as
**CGL** = after Chew, Goldberger, Low 1956
(CGL = collisionless magnetohydrodynamics)

$$\frac{\partial \rho}{\partial t} + \nabla \cdot (\rho \boldsymbol{u}) = 0;$$
$$\frac{\partial \boldsymbol{u}}{\partial t} + \boldsymbol{u} \cdot \nabla \boldsymbol{u} + \frac{1}{\rho} \nabla \cdot \boldsymbol{p} - \frac{1}{4\pi\rho} (\nabla \times \boldsymbol{B}) \times \boldsymbol{B} = 0;$$
$$\frac{\partial p_{\|}}{\partial t} + \nabla \cdot (p_{\|} \boldsymbol{u}) + 2 p_{\|} \hat{\boldsymbol{b}} \cdot \nabla \boldsymbol{u} \cdot \hat{\boldsymbol{b}} = 0;$$
$$\frac{\partial p_{\perp}}{\partial t} + \nabla \cdot (p_{\perp} \boldsymbol{u}) + p_{\perp} \nabla \cdot \boldsymbol{u} - p_{\perp} \hat{\boldsymbol{b}} \cdot \nabla \boldsymbol{u} \cdot \hat{\boldsymbol{b}} = 0;$$
$$\frac{\partial \boldsymbol{B}}{\partial t} = \nabla \times (\boldsymbol{u} \times \boldsymbol{B}).$$

$\Longleftrightarrow$

$$\frac{d}{dt} \left( \frac{p_{\|} |\boldsymbol{B}|^2}{\rho^3} \right) = 0;$$
$$\frac{d}{dt} \left( \frac{p_{\perp}}{\rho |\boldsymbol{B}|} \right) = 0.$$

Can be interpreted as conservation laws for: second adiabatic invariant (conservation of the average parallel momentum of a particle that is completely trapped and periodically bouncing inside of a magnetic bottle)

*first adiabatic invariant*
(conservation of the magnetic moment of a particle that is periodically gyrating around a mean magnetic field)

**FLR = Finite Larmor Radius (corrections)**

We define four generalized fluid models, that include the following dispersive effects :

Hall-CGL = Hall term is included in the induction equation;
FLR1 = quasi-static stress-tensor (collisionless viscosity-tensor) is included;
FLR2 = first-order time-derivative d/dt of stress-tensor is included;
FLR3 = heat fluxes are included and are *coupled* with stress-tensors,
i.e. heat fluxes enter stress-tensor, and stress-tensor enters heat fluxes

# Linearized, normalized & Fourier transformed equations in the x-z plane

Temperature anisotropy

$$a_p = \frac{T_\perp^{(0)}}{T_\parallel^{(0)}} = \frac{p_\perp^{(0)}}{p_\parallel^{(0)}}$$

$$v_{A\parallel}^2 \equiv 1 + \frac{\beta_\parallel}{2}(a_p - 1)$$

normalized parallel Alfven speed

density eq.

momentum eq.

induction eq.

pressure eqs.

$$
\begin{aligned}
&-\omega\rho + k_\perp u_x + k_\parallel u_z = 0;\\
&-\omega u_x + \frac{\beta_\parallel}{2} k_\perp p_\perp - v_{A\parallel}^2 k_\parallel B_x + k_\perp B_z + \frac{\beta_\parallel}{2}(k_\perp \Pi_{xx} + k_\parallel \Pi_{xz}) = 0;\\
&-\omega u_y - v_{A\parallel}^2 k_\parallel B_y + \frac{\beta_\parallel}{2}(k_\perp \Pi_{xy} + k_\parallel \Pi_{yz}) = 0;\\
&-\omega u_z + \frac{\beta_\parallel}{2} k_\parallel p_\parallel + \frac{\beta_\parallel}{2}(1-a_p) k_\perp B_x + \frac{\beta_\parallel}{2} k_\perp \Pi_{xz} = 0;\\
&-\omega B_x - k_\parallel u_x - i k_\parallel^2 B_y = 0;\\
&-\omega B_y - k_\parallel u_y - i k_\parallel k_\perp B_z + i k_\parallel^2 B_x = 0;\\
&-\omega B_z + k_\perp u_x + i k_\parallel k_\perp B_y = 0;\\
&-\omega p_\parallel + k_\perp u_x + 3 k_\parallel u_z + \cancel{k_\parallel q_\parallel} + k_\perp (S_\perp^\parallel)_x = 0;\\
&-\omega p_\perp + 2 a_p k_\perp u_x + a_p k_\parallel u_z + \cancel{k_\parallel q_\perp} + k_\perp (S_\perp^\perp)_x = 0,
\end{aligned}
\qquad (543)
$$

components of the stress-tensor

Hall term

gyrotropic heat fluxes (neglected)

non-gyrotropic heat flux vectors

where each component of the (FLR) pressure tensor $\boldsymbol{\Pi}$, and each component of the (FLR) heat flux vectors $\boldsymbol{S}_\perp^\parallel$, $\boldsymbol{S}_\perp^\perp$, is separated to

$$\boldsymbol{\Pi} = \boldsymbol{\Pi}^{(1)} + \boldsymbol{\Pi}^{(2)}; \qquad \boldsymbol{S}_\perp^\parallel = \boldsymbol{S}_\perp^{\parallel(1)} + \boldsymbol{S}_\perp^{\parallel(2)}; \qquad \boldsymbol{S}_\perp^\perp = \boldsymbol{S}_\perp^{\perp(1)} + \boldsymbol{S}_\perp^{\perp(2)}.$$

The components of the $\boldsymbol{\Pi}$ tensor are given by

Heat fluxes enter stress tensor

FLR1

$$
\begin{aligned}
\Pi_{xx}^{(1)} &= -\tfrac{a_p}{2} i k_\perp u_y; & \Pi_{xx}^{(2)} &= +i\tfrac{\omega}{2}\Pi_{xy}^{(1)} - i\tfrac{k_\perp}{4}(S_\perp^\perp)_y^{(1)+(2)};\\
\Pi_{xy}^{(1)} &= \tfrac{a_p}{2} i k_\perp u_x; & \Pi_{xy}^{(2)} &= -i\tfrac{\omega}{2}\Pi_{xx}^{(1)} + i\tfrac{k_\perp}{4}(S_\perp^\perp)_x^{(2)};\\
\Pi_{xz}^{(1)} &= -(2-a_p) i k_\parallel u_y; & \Pi_{xz}^{(2)} &= +i\omega\Pi_{yz}^{(1)} + (1-a_p)(\nabla\times\boldsymbol{E}_H)_y - i k_\parallel (S_\perp^\parallel)_y^{(1)+(2)};\\
\Pi_{yz}^{(1)} &= (2-a_p) i k_\parallel u_x + a_p i k_\perp u_z; & \Pi_{yz}^{(2)} &= -i\omega\Pi_{xz}^{(1)} - (1-a_p)(\nabla\times\boldsymbol{E}_H)_x + \cancel{i k_\perp q_\perp} + i k_\parallel (S_\perp^\parallel)_x^{(1)+(2)},
\end{aligned}
\qquad (544)
$$

where the Hall electric field contributions for cold massless electrons read

FLR2

$$(\nabla\times\boldsymbol{E}_H)_x = +k_\parallel^2 B_y; \qquad (\nabla\times\boldsymbol{E}_H)_y = k_\parallel k_\perp B_z - k_\parallel^2 B_x, \qquad (545)$$

and the components of the non-gyrotropic (FLR) heat fluxes are given by

Stress-tensor enters heat fluxes

FLR3

$$
\begin{aligned}
(S_\perp^\parallel)_x^{(1)} &= -\beta_\parallel (1-a_p) i k_\parallel B_y; & (S_\perp^\parallel)_x^{(2)} &= +i\omega (S_\perp^\parallel)_y^{(1)} - \beta_\parallel i k_\parallel \Pi_{yz}^{(1)};\\
(S_\perp^\parallel)_y^{(1)} &= a_p \tfrac{\beta_\parallel}{2} i k_\perp (p_\parallel - \rho) + \beta_\parallel (1-a_p) i k_\parallel B_x; & (S_\perp^\parallel)_y^{(2)} &= -i\omega (S_\perp^\parallel)_x^{(1)} + \beta_\parallel i k_\parallel \Pi_{xz}^{(1)};\\
(S_\perp^\perp)_x^{(1)} &= 0; & (S_\perp^\perp)_x^{(2)} &= +i\omega (S_\perp^\perp)_y^{(1)} - a_p \tfrac{\beta_\parallel}{2} i k_\perp \Pi_{xy}^{(1)};\\
(S_\perp^\perp)_y^{(1)} &= \beta_\parallel a_p i k_\perp (p_\perp - a_p\rho); & (S_\perp^\perp)_y^{(2)} &= -\cancel{i\omega (S_\perp^\perp)_x^{(1)}} + a_p \tfrac{\beta_\parallel}{2} i k_\perp \Pi_{xx}^{(1)}.
\end{aligned}
\qquad (546)
$$

**Growth rates of firehose instabilities**

*Hunana et al. 2019 (Part 1)*

direction of propagation

wavenumber

*Note the differences in legends, huge **enhancement** for FLR3 model*

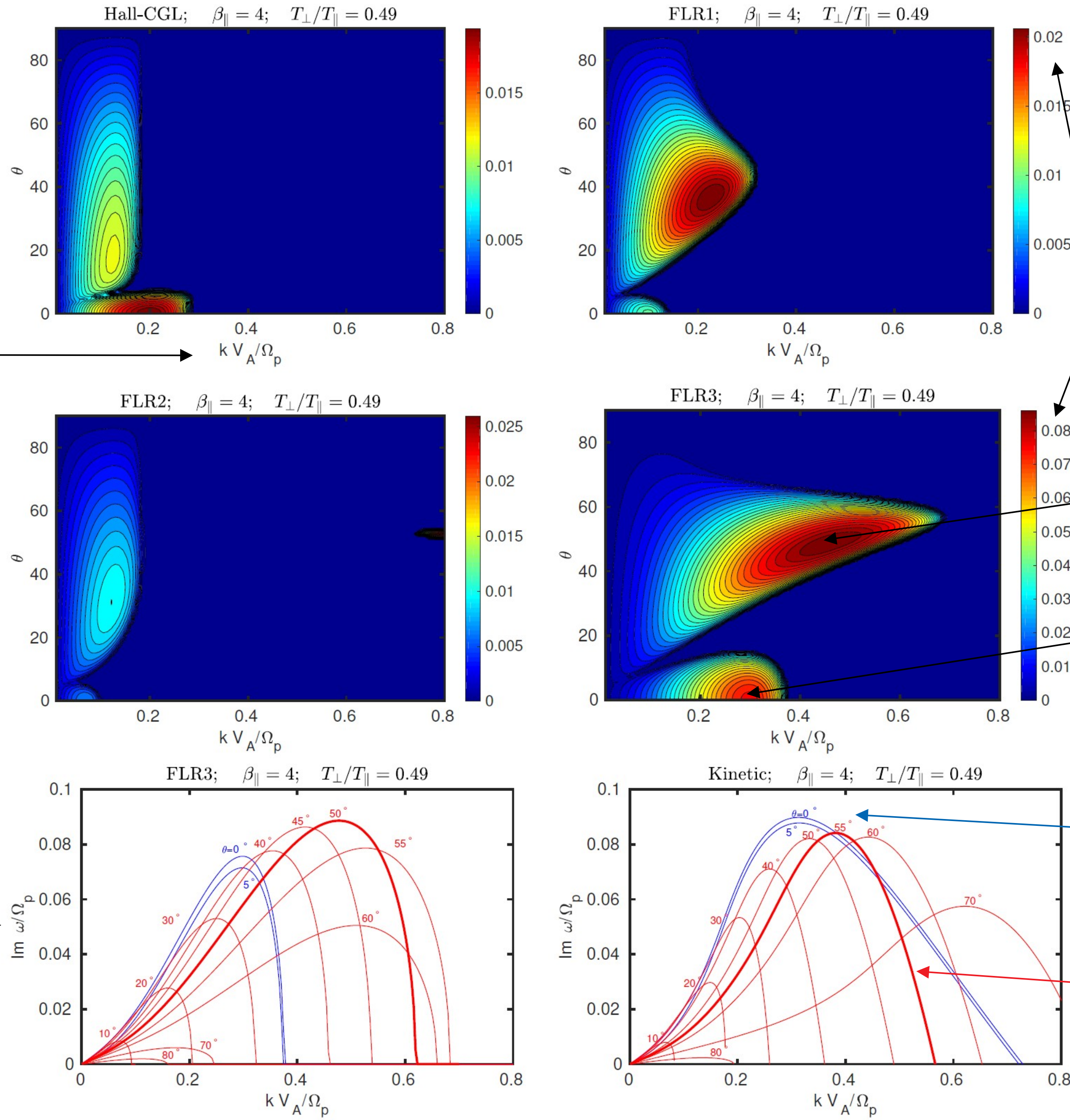


Oblique firehose

Parallel firehose

Growth rates for several directions of propagation

Parallel firehose

Oblique firehose

Not perfect, but surprisingly close !

**Figure 10.** The growth rate plotted in the $(k, \theta)$ plane, with fixed $\beta_\parallel = 4$ and $a_p = 0.49$ (the hard firehose threshold is at $a_p = 0.5$), showing the parallel and oblique firehose instability. Four different fluid models are plotted. Top left: Hall-CGL; top right: Hall-CGL-FLR1; middle left: Hall-CGL-FLR2, middle right: Hall-CGL-FLR3. We do not provide contour plot for kinetic theory. Nevertheless, bottom figures show solutions for several propagation angles. Bottom left: Hall-CGL-FLR3 model, bottom right: kinetic.

# Parallel firehose instability

*Hunana et al. 2019 (Part 1)*

dashed lines = fluid;  solid lines = kinetic

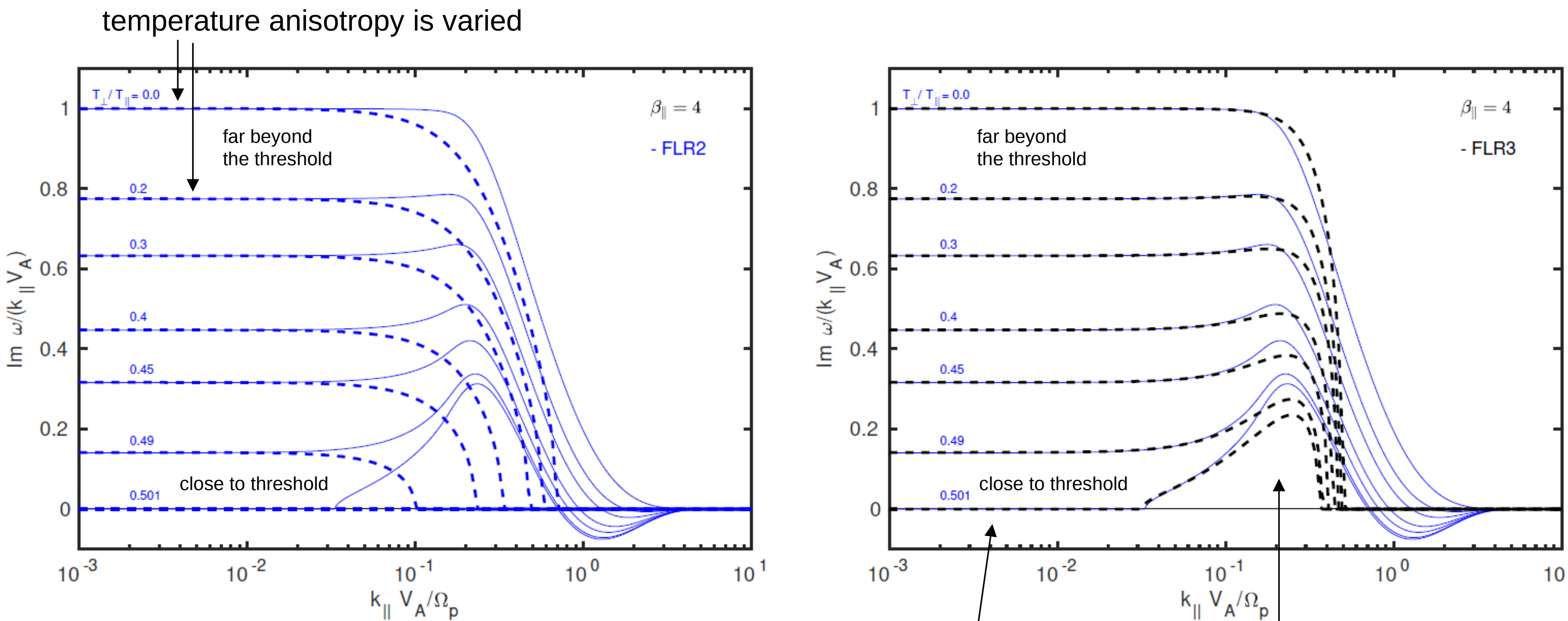


**Figure 7.** Imaginary phase speed (growth rate normalized to the wavenumber) of the parallel firehose instability. The $\beta_\parallel = 4$, and temperature anisotropy is varied so that the whistler mode is in the firehose unstable regime. Solid lines (blue) are kinetic solutions, obtained with the WHAMP code. Dashed lines are fluid solutions. Left figure: FLR2 solutions (blue), Right figure: FLR3 solutions (black). It is shown that in contrast to the FLR2 model, the FLR3 model reproduces the large "bump" when close to the long-wavelength "hard" firehose threshold $T_\perp/T_\parallel = 0.5$.

Stable at long wavelengths

Unstable at short wavelengths

It shows that fluids, similarly to kinetic theory, can become firehose-unstable at short wavelengths, while being stable in the long-wavelength limit.

# Examples of matching the kinetic theory with fluid description

1) Dispersion relation for perpendicular fast mode, in the long-wavelength limit:

rho_i = Larmor radius

$$\mathrm{FLR1}: \quad \omega^2 = k_\perp^2\left[V_A^2 + v_{\mathrm{th}\perp}^2\left(1+\frac{k_\perp^2\rho_i^2}{16}\right)\right];$$

$$\mathrm{FLR2}: \quad \omega^2 = k_\perp^2\left[V_A^2\left(1-\frac{k_\perp^2\rho_i^2}{8}\right) + v_{\mathrm{th}\perp}^2\left(1-\frac{k_\perp^2\rho_i^2}{16}\right)\right];$$

note the change of sign, Del Sarto et al. 2017

$$\mathrm{Kinetic}: \quad \omega^2 = k_\perp^2\left[V_A^2\left(1-\frac{k_\perp^2\rho_i^2}{8}\right) + v_{\mathrm{th}\perp}^2\left(1-\frac{5}{16}k_\perp^2\rho_i^2\right)\right].$$

$$\mathrm{FLR3}: \quad \omega^2 = k_\perp^2\left[V_A^2\left(1-\frac{k_\perp^2\rho_i^2}{8}\right) + v_{\mathrm{th}\perp}^2\left(1-\frac{5}{16}k_\perp^2\rho_i^2\right)\right].$$

complete match, first shown by Mikhailovskii & Smolyakov 1985

2) Damping of parallel sound (ion-acoustic) mode in a collisionless regime. It is caused by the Landau damping, and requires **Landau fluid models**, not discussed here. Similarly, damping of the electron Langmuir mode.

PHYSICAL REVIEW LETTERS **121,** 135101 (2018)

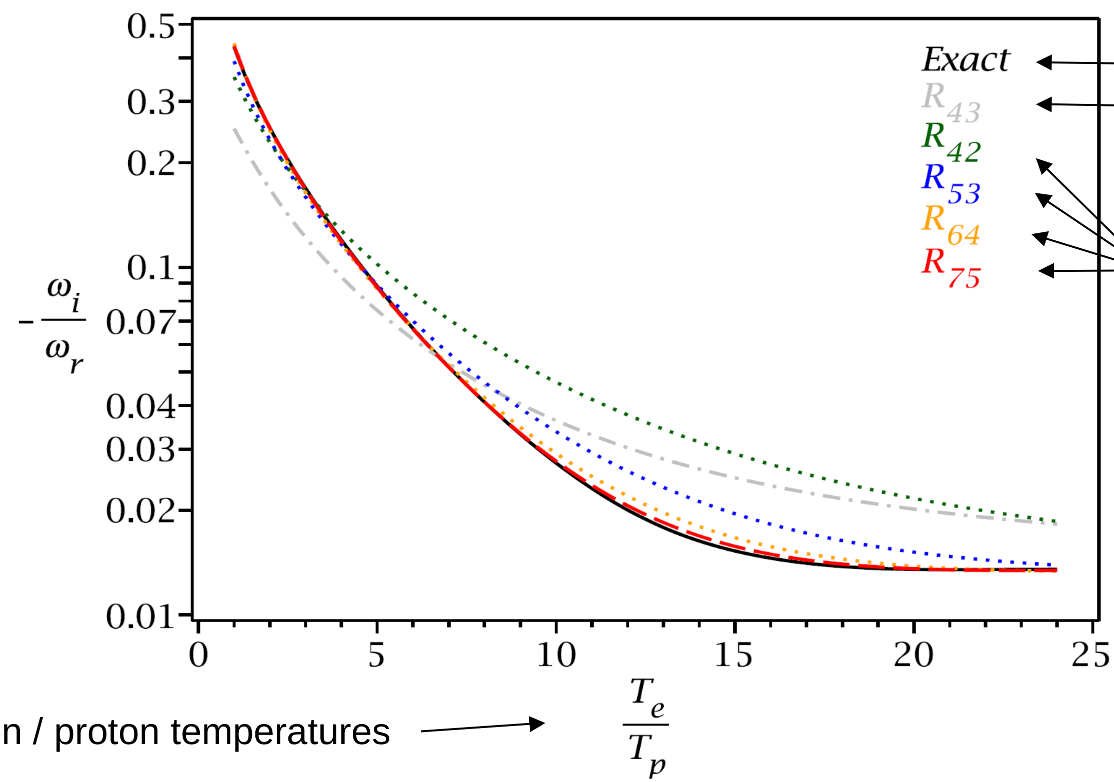


Damping of the sound mode / its real frequency

Ratio of electron / proton temperatures

kinetic theory

Hammett and Perkins 1990

Hunana et al. 2018, convergence of fluid and kinetic descriptions was shown

If you are interested in collisionless fluid models and want to explore how to incorporate kinetic effects into a fluid description, there exists a detailed introductory guide.

The most comprehensive review of CGL-type models is Part 1:

*J. Plasma Phys.* (2019), *vol.* 85, 205850602 https://arxiv.org/abs/1901.09354

**An introductory guide to fluid models with anisotropic temperatures. Part 1. CGL description and collisionless fluid hierarchy**

P. Hunana[1,2,†], A. Tenerani[3], G. P. Zank[4,5], E. Khomenko[1,2], M. L. Goldstein[6], G. M. Webb[4], P. S. Cally[7], M. Collados[1,2], M. Velli[8] and L. Adhikari[4]

The most comprehensive review of Landau fluid models is Part 2:

*J. Plasma Phys.* (2019), *vol.* 85, 205850603 https://arxiv.org/abs/1901.09360

**An introductory guide to fluid models with anisotropic temperatures. Part 2. Kinetic theory, Padé approximants and Landau fluid closures**

P. Hunana[1,2,†], A. Tenerani[3], G. P. Zank[4,5], M. L. Goldstein[6], G. M. Webb[4], E. Khomenko[1,2], M. Collados[1,2], P. S. Cally[7], L. Adhikari[4] and M. Velli[8]